Dynamic Simulations of Combined Transmission and Distribution Systems using Decomposition and Localization

Petros Aristidou
Department of Electrical Engineering
and Computer Science
University of Liège, Belgium
p.aristidou@ieee.org

Thierry Van Cutsem
Fund for Scientific Research (FNRS) at
Department of Electrical Engineering
and Computer Science
University of Liège, Belgium
t.vancutsem@ulg.ac.be

Abstract—**Simulating a power system with both transmission and distribution networks modeled is a challenging task. On the one hand, it is difficult to set up equivalents restituting the dynamic behavior of aggregated loads and distributed generation units. On the other hand, representing all distribution networks in detail is computationally very demanding. In this paper, the combination of a domain-decomposition approach with the exploitation of the localized nature of power system responses to disturbances is proposed. Distribution networks marginally participating to the system dynamics are automatically replaced by simple models, while the others are simulated with full detail, thereby preserving simulation accuracy.**

Index Terms—**time-domain simulation, active distribution networks, domain decomposition methods, localization**

I. Introduction

The most noticeable developments foreseen in power systems involve Distribution Networks (DNs). Future DNs are expected to host a big percentage of the renewable energy sources and play a key role in the development of future grids. The resulting challenge in dynamic simulation is to correctly represent DNs and their participation in system dynamics. This becomes compulsory as DNs are called upon to actively support the Transmission Network (TN) with an increasing number of Distributed Generation Units (DGUs) and active loads participating in ancillary services through smart-grid technologies.

In present-day dynamic security assessment of a large-scale power system, it is common to represent the bulk generation and higher voltage (transmission) levels accurately, while the lower voltage (distribution) levels are equivalenced. On the other hand, when concentrating on a DN, the TN is often represented by a Thévenin equivalent. The prime motivation behind this practice has been the lack of computational resources. Indeed, fully representing the entire power system network was simply impossible given the available computing equipment (memory capacity, processing speed, etc.). Even with current computational resources this task is extremely challenging. Each DN can easily include hundreds if not thousands of buses, loads, and branches. Handling a model with hundreds of thousands of TN and DN variables proves impossible with traditional simulation algorithms.

As modern DNs are evolving with power-electronics interfaces, DGUs, active loads, and control schemes, more detailed and elaborate equivalent models would be needed to encompass the dynamics of DNs and their impact on global system dynamics. The three main equivalencing approaches reported in the literature are modal methods, coherency methods and measurement or simulation-based methods [1]. Equivalent models, however, suffer from a number of drawbacks:

- the identity of the replaced system is lost. Faults that happen inside the DNs themselves cannot be simulated and individual voltages at internal buses, currents, controllers, etc. cannot be observed anymore;
- most equivalent models target a specific type of dynamics (short-term, long-term, electromechanical oscillations, voltage recovery, etc.) and fail when used for another type. This requires running different types of simulations with different models;
- in most cases, the use or not of these equivalent models is decided off-line, when it is still unknown whether the disturbance will affect or not the DNs of concern.

In this paper a method is proposed for performing faster dynamic simulations of combined transmission and distribution networks while preserving simulation accuracy. The proposed method consists in representing in detail the DNs actively participating to the system dynamics (called *active*) while the remaining DNs (called *latent*) are replaced automatically, during the simulation, by much smaller models.

II. Model decomposition

Let the power system be decomposed into the TN, the DNs and a number of components connected to them, as sketched in Fig. 1 [2]. For reasons of simplicity, all the components connected to the TN or DNs that either produce or consume power in normal operating conditions (such as power plants, DGUs, induction motors, other loads, etc.) are called *injectors*.
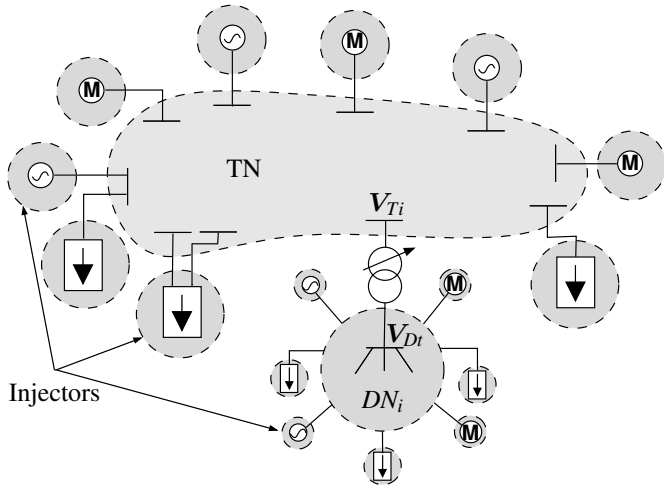
Figure 1. Decomposed Power System

The injectors are described by a system of non-linear Differential-Algebraic Equations (DAEs) [3]:

$$\boldsymbol{\Gamma}\dot{\boldsymbol{x}} = \boldsymbol{\Phi}(\boldsymbol{x}, \boldsymbol{V})$$

where $\boldsymbol{V}$ is the vector of voltages ($\boldsymbol{V}_{Di}$ if connected to the i-th DN or $\boldsymbol{V}_T$ if connected to the TN, see Fig. 1), $\boldsymbol{x}$ is the state vector containing differential and algebraic variables of the injectors and $\boldsymbol{\Gamma}$ is a diagonal matrix with

$$(\boldsymbol{\Gamma})_{\ell\ell} = \begin{cases} 0 & \text{if the } \ell\text{-th equation is algebraic} \\ 1 & \text{if the } \ell\text{-th equation is differential.} \end{cases}$$

Under the standard phasor approximation, the algebraic equations of each network (TN or DN) take on the linear form:

$$0 = \boldsymbol{D}\boldsymbol{V} - \boldsymbol{I} = \boldsymbol{g}(\boldsymbol{x}, \boldsymbol{V})$$

Hence, the full DAE system describing the TN is:

$$\begin{aligned} \boldsymbol{0} &= \boldsymbol{g}_T(\boldsymbol{x}_T, \boldsymbol{V}_T, \boldsymbol{V}_{Dt}) \\ \boldsymbol{\Gamma}_T\dot{\boldsymbol{x}}_T &= \boldsymbol{\Phi}_T(\boldsymbol{x}_T, \boldsymbol{V}_T) \end{aligned} \quad (1)$$

where $\boldsymbol{x}_T$ (the state vector of injectors connected to the TN) and $\boldsymbol{V}_T$ (the vector of TN voltages) are internal variables, while $\boldsymbol{V}_{Dt}$ (the vector of DN voltages connected to a TN bus, see Fig. 1) are external variables.

Similarly, for the i-th DN ($i = 1, \ldots, N$):

$$\begin{aligned} \boldsymbol{0} &= \boldsymbol{g}_{Di}(\boldsymbol{x}_{Di}, \boldsymbol{V}_{Di}, V_{Ti}) \\ \boldsymbol{\Gamma}_{Di}\dot{\boldsymbol{x}}_{Di} &= \boldsymbol{\Phi}_{Di}(\boldsymbol{x}_{Di}, \boldsymbol{V}_{Di}) \end{aligned} \quad (2)$$

where $\boldsymbol{x}_{Di}$ and $\boldsymbol{V}_{Di}$ are internal variables and V_{Ti} (the voltage of the TN bus the DN is connected to) is external.

To simulate the combined TN and DNs system two main families of methods can be employed.

On the one hand, an integrated scheme can be used. In this case, the DAE systems (1) and (2) are solved together. After time has been discretized and differential equations have been algebraized, the whole set of algebraic equations is solved by Newton method to compute all states at each discrete time instant. This is a well-known method used by many commercial and academic software.

On the other hand, a decomposed scheme can be used. In this case, each of the DAE systems (1) and (2) is solved separately and the interface variables, that is $\boldsymbol{V}_{Dt}$ for (1) and V_{Ti} for (2), are exchanged. Several decomposed schemes have been proposed in literature differing mainly by the method of exchanging interface variables. The most prominent methods are: updating the interface variables after every sub-system's Newton iteration, updating the interface variables after computing a converged solution of each system of equations, or using a global reduced system to accurately compute the interface variables before each decomposed Newton iteration [2]. More information can be found in Chapter 14 of [4].

The method reported in this paper consists of replacing, during the simulation, the full DAE system (2) of a latent DN by a smaller linear model. The full model is restored if the DN becomes active again. In an integrated scheme this change between active and latent would lead to constant changes on the size and structure of the Jacobian matrix with unacceptable computational overhead in factorization operations. For this reason, a decomposed scheme is crucial to the algorithm since it gives the possibility of replacing DNs with simpler models connected to the TN without the need of recalculating and re-factorizing all the jacobian matrices involved in the decomposed system solution.

Consequently, for the implementation of the localization algorithm, the decomposed scheme presented in [2] has been extended to accommodate the solution of DNs. Summarizing here, the TN and DN systems are solved separately and a Schur complement method is used to build a reduced system and compute the interface variables ($\boldsymbol{V}_{Dt}, \boldsymbol{V}_{Ti}$) before solving each subset of linearized equations.

III. SIMPLIFIED MODEL OF LATENT DNS

The proposed method accommodates a wide range of models to account for the behavior of a DN when it is latent. It must be emphasized that the modeling requirements are low since the simplified model is used only when the DN has been characterized as latent and hence experiences low dynamic activity.

The results shown in this paper are obtained with the latent DNs replaced by a linear sensitivity model. That is, after a DN is declared latent at time t^*, the DN voltages are updated according to their sensitivity to TN voltage variations:

$$\boldsymbol{V}_D(t_n) = \boldsymbol{V}_D(t^*) - \boldsymbol{G}_D(t^*)\left[\boldsymbol{V}_T(t_n) - \boldsymbol{V}_T(t^*)\right] \quad (3)$$

for any discrete time $t_n \geq t^*$. The sensitivity matrix $\boldsymbol{G}_D$ is calculated from the full model (2) at the moment the DN switches from active to latent.

The simplified model is easy and fast to compute and incorporates the dynamic activity of a latent DN at the moment of switching. A further benefit arises from the way the interface variables ($\boldsymbol{V}_{Dt}, \boldsymbol{V}_{Ti}$) are computed in the decomposed scheme used. The contribution of both models (2) and (3) to the Schur complement (linear) system, which is used to solve for
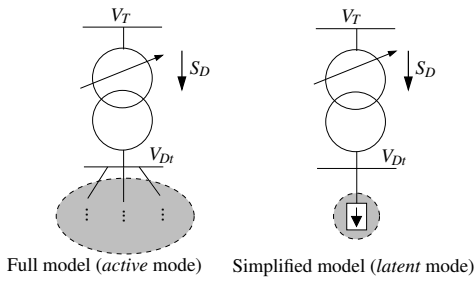
Figure 2. Representation of a DN in active and latent modes

the interface variables [2], are mathematically the same, thus alleviating the need for re-computing and re-factorizing that matrix.

IV. LATENCY CRITERION

In the context of large-scale power system dynamic simulations, DNs in the area affected by the disturbance are actively contributing to the dynamics while the remaining DNs exhibit low activity. The switching algorithm automatically selects between active and latent mode for each individual DN to speed up the simulation while preserving accuracy.

The dynamic simulation starts with the detailed models of both transmission and distribution networks and the dynamic activity of the i-th DN is quantified through the variation of the apparent power ($S_{Di} = \sqrt{P_{Di}^2 + Q_{Di}^2}$) in each distribution transformer (see Fig. 2). In short, DN_i is declared latent when its apparent power S_{Di} has "not changed significantly for some time", or, in other words, exhibits small variability. This observation variable is chosen because it incorporates the information needed on the dynamic activity of a DN and the effect it has on the remaining of the system. More detailed information for the state of the DN could be extracted from monitoring separately the active and reactive powers, but this comes to the expense of doubling the calculations and the memory needed for the latency criterion.

In more detail, the standard deviation of S_{Di} is monitored over a moving time-window. When this value gets smaller than a pre-defined tolerance ϵ_L, DN_i is declared latent. To calculate the standard deviation of S_{Di} efficiently, an approximation originating from real-time digital signal processing is used [5].

First of all, at time t_n the average is obtained as the weighted sum of the new value $S_{Di}(t_n)$ and the previous average value $S_{Di,av}(t_{n-1})$ according to:

$$S_{Di,av}(t_n) = (1 - \lambda_1) * S_{Di,av}(t_{n-1}) + \lambda_1 * S_{Di}(t_n)$$

with $0 \leq \lambda_1 \leq 1$. The parameter λ_1 sets the time window of observation for averaging, i.e. a smaller value extends the observation window while a larger curtails it.

Next, the difference between the new value and the computed average, i.e. $\triangle S_{Di}(t_n) = S_{Di}(t_n) - S_{Di,av}(t_n)$, is used to calculate the approximate variance:

$$S_{Di,var}(t_n) = (1 - \lambda_2) * S_{Di,var}(t_{n-1}) + \lambda_2 * \triangle S_{Di}(t_n)^2$$
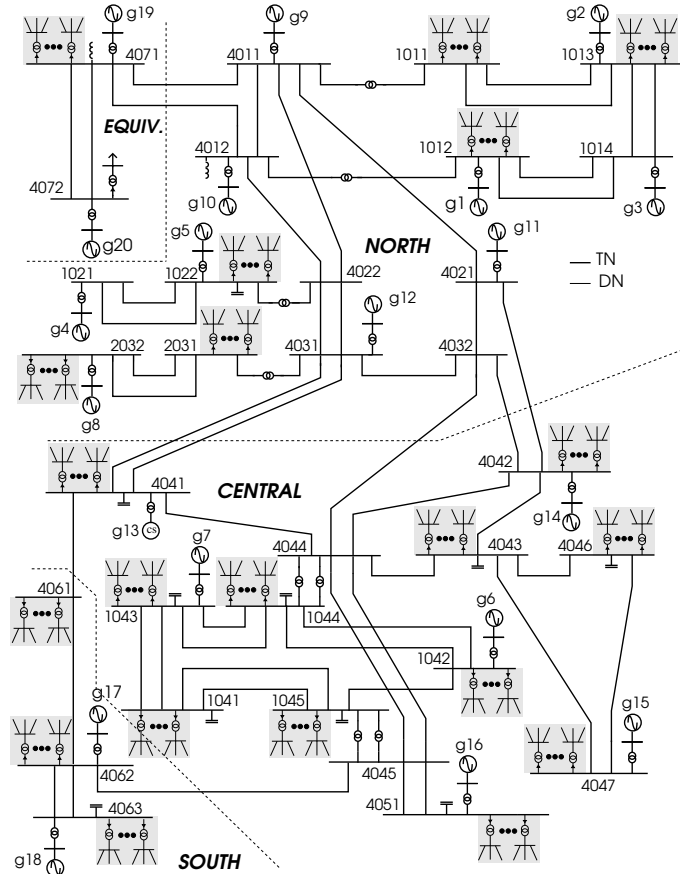

Figure 3. Expanded Nordic System

with $0 \leq \lambda_2 \leq 1$. The parameter λ_2 sets the response time to the changes $\triangle S_{Di}$, i.e. a smaller value makes the criterion less responsive.

Finally, the approximate standard deviation of S_{Di} is computed as:

$$S_{Di,std}(t_n) = \sqrt{S_{Di,var}(t_n)}$$

and is compared to ϵ_L to decide the status of the i-th DN.

More information on the metrics and the effects of parameters λ_1 and λ_2 on the latency criterion can be found in [5].

While DN_i is latent, the absolute deviation of $S_{Di}(t_n)$ from its value at the time it was declared latent $S_{Di}(t^*)$ is monitored. If the difference gets bigger than ϵ_L, the DN is considered to have moved away from its linearization point and the sensitivity model not to be an accurate representation any longer; hence, the DN is switched to active.

V. RESULTS WITH A 14653-BUS SYSTEM

This section reports on results obtained with a large-scale combined transmission and distribution network model based on the Nordic32 system (see Fig. 3). The original TN model, which is documented in [6], is extended to include 146 realistic DNs replacing the aggregated distribution loads of the original system. The model and data of each DN were taken from [7] and scaled to match the original loads. Multiple DNs were

ϵ_L (MVA)	C1				C2				C3			
	CPU Time (s)	Speedup (times)	V_{err} (pu)	S_{Derr} (%)	CPU Time (s)	Speedup (times)	V_{err} (pu)	S_{Derr} (%)	CPU Time (s)	Speedup (times)	V_{err} (pu)	S_{Derr} (%)
0.00	1326	-	-	-	1534	-	-	-	2420	-	-	-
0.01	728	1.8	1.0E-4	0.01	493	3.1	2.6E-5	0.01	1374	1.8	1.9E-4	0.01
0.05	353	3.8	1.2E-4	0.05	307	5.0	5.0E-4	0.08	965	2.5	3.8E-3	0.04
0.08	293	4.5	1.3E-4	0.08	261	5.9	1.1E-3	0.14	950	2.5	3.8E-3	0.06
0.10	277	4.8	1.9E-4	0.12	256	6.0	1.4E-3	0.23	857	2.8	6.0E-3	0.10
0.50	176	7.5	7.1E-4	0.69	203	7.6	2.8E-3	0.24	578	4.2	7.7E-3	0.25

used to match the original load powers, taking into account the nominal power of the DN transformers.

The TN includes 53 buses, 222 branches, 20 synchronous machines represented in detail together with their excitation systems, voltage regulators, power system stabilizers, speed governors and turbines.

Each one of the 146 DNs includes 100 buses, 108 branches, one Distribution Voltage Regulator (DVR) equipped with Load Tap Changing (LTC) device, three type-1 and three type-2 Wind Turbines (WTs) [8], 12 impedance loads and 133 dynamically modeled loads, such as, small induction machines and self-restoring exponential loads. The transformer connecting each DN to the TN is also equipped with an LTC controlling the distribution side voltage (as shown in Fig. 2).

Moreover, to avoid identical DNs and artificial synchronization, the delays on transformer tap changes were randomized around their original values and the WTs were randomly initialized to produce 60 to 100% of their nominal power.

In total, the combined transmission and distribution system includes 14653 buses, 15990 branches, 20 synchronous machines, 293 LTC equipped transformers, 876 wind-turbines, 1752 impedance loads and 19419 dynamically modeled loads. The resulting DAE system has 137742 states.

Finally, the latency criterion presented in Section IV was used with $\lambda_1 = \lambda_2 = 0.01$ and ϵ_L varying between zero (fully accurate simulation) and 0.5 MVA. Two metrics are used to quantify the error introduced by the algorithm. First, the maximum average error on voltage:

$$V_{err} = \max_{i=1...M} \left[\frac{1}{n_s} \sum_{k=1}^{n_s} |V_i(k,\epsilon_L) - V_i(k,0)| \right]$$

with M the number of all buses of the system and n_s the number of time-steps taken during the simulation. Second, the maximum average error on DN apparent power:

$$S_{Derr} = \max_{i=1...N} \left[\frac{1}{n_s} \sum_{k=1}^{n_s} \left| \frac{S_{Di}(k,\epsilon_L) - S_{Di}(k,0)}{S_{Di}(k,0)} \right| \right]$$

A. Case C1

The disturbance considered in C1 is the loss of approximately 90 MW of wind generation due to the disconnection of 30 type-1 and 30 type-2 WTs located inside the DNs connected to TN bus 1041 in the CENTRAL area (see Fig. 3). The 60 WTs are disconnected over a period of 2 s and the system is simulated for 140 s with a time-step of 1 cycle at the nominal
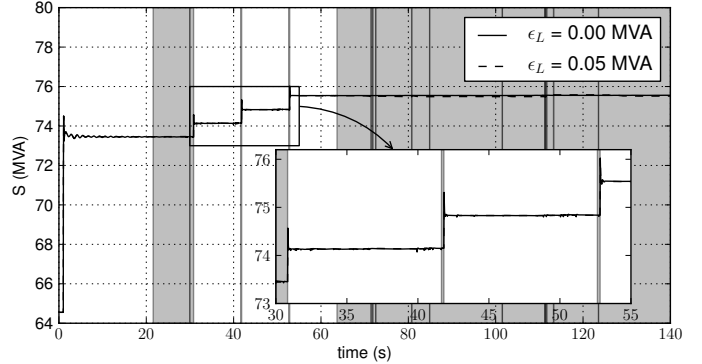

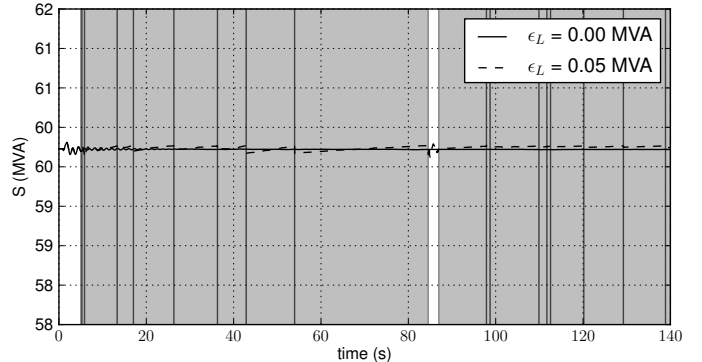Figure 4. Case C1: Apparent power into disturbed DN (on TN bus 1041)

Figure 5. Case C1: Apparent power into a remote DN (on TN bus 1011)

frequency (50 Hz). The DNs compensate by importing more power from the TN. Such an event might result from high winds in the area, causing WTs to trip to avoid damage.

This event affects mainly the DNs in the CENTRAL area, while DNs located far away (NORTH and SOUTH areas) are barely affected. Such disturbances, with events happening inside the DNs, are very difficult - if not impossible - to simulate when DN models are fully equivalenced beforehand.

Table I shows the speedup from increasing ϵ_L, ranging from 1.8 to 7.5 times, and the error V_{err} ranging from $1.0E-4$ pu to $7.1E-4$ pu and S_{Derr} from 0.01% to 0.69%.

Figure 4 displays S_D into one of the disturbed DN with the latent periods shown in gray and the vertical lines signaling the transition between modes. As expected, at the end of the simulation the DN imports more power compared to the pre-disturbance state to compensate for the lost WT generation.
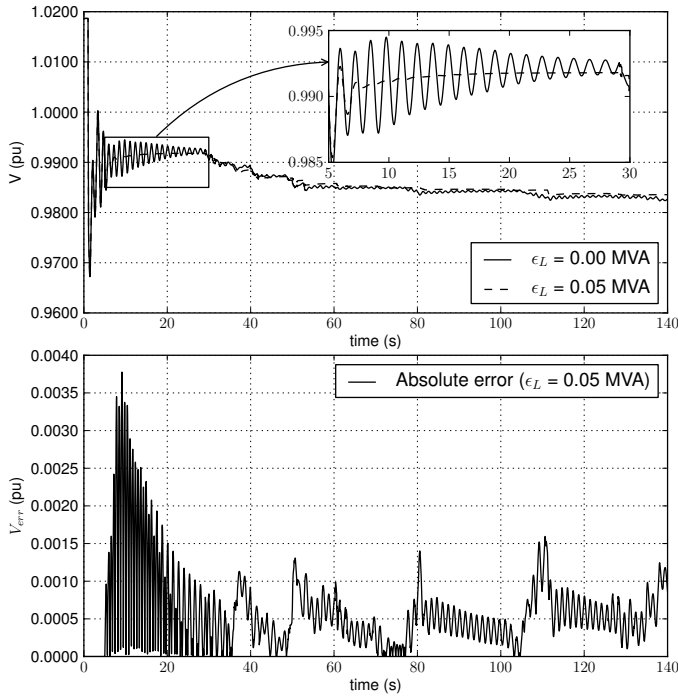
Figure 6. Case C1: Voltage evolution at bus 1041 and corresponding absolute error

Figure 7. Case C2: Apparent power into nearby DN (on TN bus 1011)

Figure 8. Case C2: Apparent power into a remote DN (on TN bus 1045)

The effect of the distribution transformer LTC device restoring the voltage level in the DN can be also seen.

Additionally, Fig. 5 displays S_D into a remote DN located in the NORTH area and connected to TN bus 1011. As can be seen, the remote DN remains almost unaffected by the disturbance. The DN becomes latent much earlier and remains latent almost through the whole situation. In both figures, the accurate and with latency $\epsilon_L = 0.05$ MVA curves are almost indiscernible (see zoom in Fig. 4).

Moreover, Fig. 6 shows the voltage evolution and absolute voltage error $|V(k, \epsilon_L) - V(k, 0)|$ at bus 1041, the TN bus closest to the disturbance. The sudden voltage drop during the event, as well as the further gradual voltage decrease stemming from LTC actions can be observed. From the same figure, it is seen that the biggest discrepancy between the two voltage evolutions never exceeds 0.004 pu.

B. Case C2

The disturbance considered in this case is the loss of generator $g9$ located in the NORTH region and producing approximately 400 MW and 100 MVAr. The system is simulated for 240 s with the same time step as in case C1. This disturbance affects mainly the NORTH area, close to the tripped generator.

Table I shows the speedup, ranging from 3.1 to 7.6 times, and the errors V_{err} and S_{Derr}, which are minimal for all ϵ_L values considered.

Figure 7 displays S_D into a DN situated close to the tripped generator while Fig. 8 refers to a remote DN in CENTRAL area. As expected, the nearby DN gets more affected by the
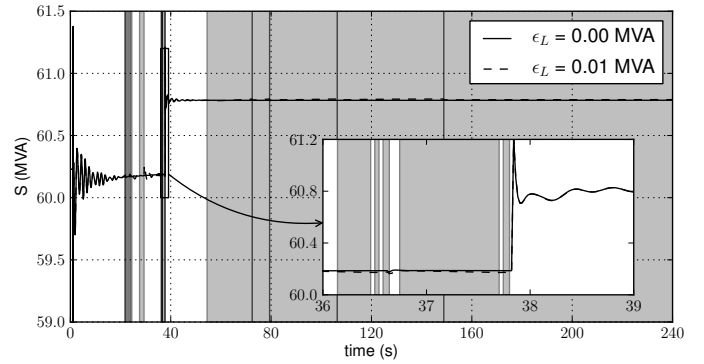
disturbance while the remote DN remains almost unaffected and latent for longer period.

Finally, Fig. 9 shows the absolute voltage error on the nearby TN bus 1011 located in the NORTH area. It barely exceeds 0.0002 pu.

C. Case C3

The disturbance considered in case C3 is a 5-cycle (0.1 s) short circuit near the TN bus 4032 cleared by the opening line $4032 - 4042$. The system is then simulated over 240 s with a one-cycle time-step. The system evolves in the long term under the effect of the LTCs and overexcitation limiters on the generators. This is a severe disturbance that affects all the TN and DNs.
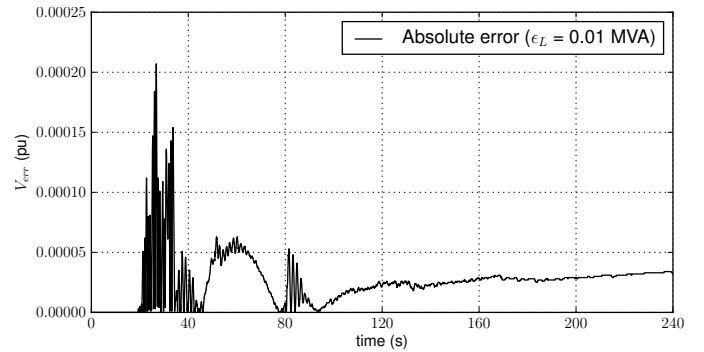

Figure 9. Case C2: Absolute voltage error near the disturbance (TN bus 1011)
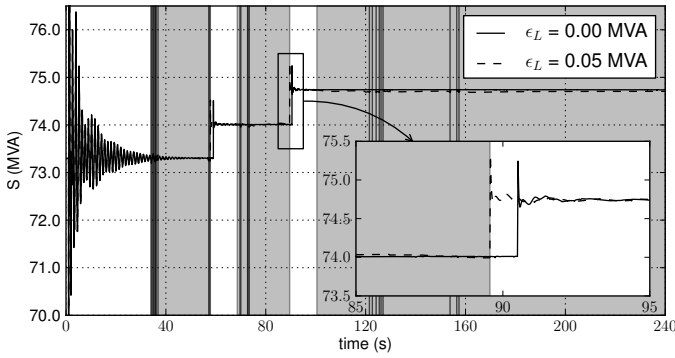
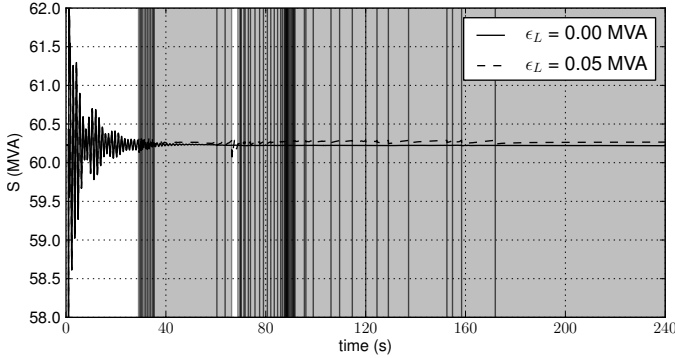Figure 10. Case C3: Apparent power into nearby DN (on TN bus 4042)

Figure 11. Case C3: Apparent power into a remote DN (on TN bus 1013)

Table I shows the speedup, ranging from 1.8 to 4.2 times, and the errors V_{err} and S_{Derr} are negligible for all ϵ_L values considered. Due to the severity of the disturbance and the effect it has on the whole system, the speedup is significantly lower than the previous, more localized, cases.

Figure 10 displays S_D into a DN situated in the area strongly affected by the disturbance. The two evolutions (accurate and with latency) are almost indiscernible for most of the simulation except around 90 s (see zoom in Fig. 10). This discrepancy is due to the delayed by one second action of the distribution transformer LTC device. LTC devices are discrete with response times in the order of 10 seconds; therefore, the above delay has small practical consequence.
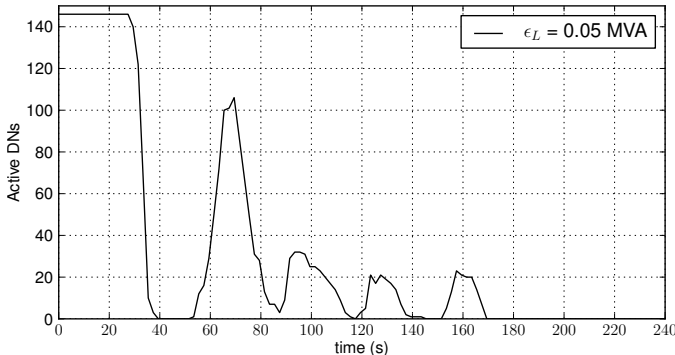

Figure 12. Case C3: Active DNs during simulation

Moreover, Fig. 11 displays S_D into a remote DN where the effect of the disturbance is less severe. Hence, the DN turns latent faster and gets back to active mode for short periods of time.

Finally, Fig. 12 shows the overall DN activity in the system during the simulation. Significant activity is observed during the first 35 s with all DNs remaining active. This is followed by a small period of inactivity where all the DNs become latent. Then, the DVR devices inside the DNs, with an initial response time of approximately 60 s, start acting and many DNs become active again. The following period until 170 s is dominated by the distribution transformer and DVR responses which periodically "wake up" several latent distribution networks. In the final period, following 170 s, all LTC-controlled voltages are restored in their dead-bands and all the DNs become latent.

VI. Conclusion

In the future, the rising need for simulating larger power system models, including DNs, will further increase the computational burden of dynamic simulations. Distributed protection and control schemes, DGUs providing ancillary services and active demand response will make the contribution of DNs to the system dynamics more significant and the exploitation of localization techniques for performance more vital.

This paper presents a method relying on a transmission-distribution system decomposition, and exploiting the localized response of distribution sub-systems to perform large-scale dynamic simulations of the whole system.

Detailed (unreduced) models are used for the active DNs to preserve accuracy, while the simulation is speeded up by substituting the DNs not participating in the system dynamics with simplified, small and linear models. The effectiveness and accuracy of the proposed algorithm was demonstrated by simulating several disturbances on a 14653-bus system including both transmission and distribution networks.

References

[1] U. D. Annakkage, N. K. C. Nair, Y. Liang, A. M. Gole, V. Dinavahi, B. Gustavsen, T. Noda, H. Ghasemi, A. Monti, M. Matar, R. Iravani, and J. A. Martinez, "Dynamic System Equivalents: A Survey of Available Techniques," *IEEE Trans. Power Delivery*, vol. 27, no. 1, pp. 411–420, Jan. 2012.

[2] D. Fabozzi, "Decomposition, Localization and Time-Averaging Approaches in Large-Scale Power System Dynamic Simulation," Ph.D. dissertation, University of Liège, 2012. [Online]. Available: http://hdl.handle.net/2268/126720

[3] P. Kundur, *Power system stability and control*. McGraw-hill New York, 1994.

[4] Y. Saad, *Iterative methods for sparse linear systems*, 2nd ed. Society for Industrial and Applied Mathematics, 2003.

[5] P. Aristidou, D. Fabozzi, and T. Van Cutsem, "Exploitation of localization for fast power system dynamic simulations," in *Paper submitted for presentation at Power Tech 2013 conference*.

[6] T. Van Cutsem, "Description, modeling and simulation results of a test system for voltage stability analysis," University of Liège, Internal report, 2013. [Online]. Available: http://hdl.handle.net/2268/141234

[7] A. Ishchenko, "Dynamics and stability of distribution networks with dispersed generation," Ph.D. dissertation, Dept. Electrical. Eng., Univ. TU/ E, the Netherlands, 2008.

[8] A. Ellis, Y. Kazachkov, E. Muljadi, P. Pourbeik, and J. Sanchez-Gasca, "Description and technical specifications for generic wtg models: A status report," in *Power Systems Conference and Exposition (PSCE), 2011 IEEE/PES*, march 2011, pp. 1 –8.